MECHANICAL TUNING OF MAGNETIC ANISOTROPY

Mustafa Mert Torunbalci and Sunil Ashok Bhave
OxideMEMS Lab, Purdue University, West Lafayette, USA

ABSTRACT

This paper demonstrates piezo-mechanical manipulation of magnetic anisotropy in a thin-film CoFeB ferromagnet (FM) via magnetostriction effect. A 20 nm thick CoFeB resistor is fabricated at the base of an AlN cantilever and its magnetization change is detected by measuring anisotropic magnetoresistance (AMR). The uniaxial strain induced in the CoFeB strip by cantilever bending exhibits a 22% change in AMR and rotates the magnetic anisotropy by 20°.

KEYWORDS

AMR, AlN actuator, magnetostriction

INTRODUCTION

Intel recently proposed magneto-electric spin-orbit (MESO) spintronic logic and memory technology as a beyond-CMOS replacement for ultra-low-power microprocessors [1]. The key MESO component is a charge-to-spin magnetoelectric transducer made using $BiFeO_3$. Although $BiFeO_3$ is a worthy candidate as an intrinsic multiferroic material [2], composite multiferroics formed by coupling magnetostrictive ferromagnet (FM) and piezoelectric films have distinct advantages such as sputtered film deposition, low thermal budget and established recipes for deposition and etching [3].

In order to achieve magnetostrictive effect, it is needed to generate an in-plane anisotropic strain on the ferromagnet [4-9]. However, PZT and AlN thin-films do not have such behavior since they have isotropic in-plane piezoelectric coefficients. But a MEMS cantilever can achieve anisotropic strain because of preferential bending direction [10].

In this work, we utilize the uniaxial strain generated by an AlN MEMS cantilever to manipulate magnetic anisotropy of CoFeB ferromagnets via magnetostriction effect. A thin-film CoFeB ferromagnetic strip is fabricated at the base of an AlN cantilever. The mechanical bending of the AlN cantilever generates in-plane unidirectional strain at the base which is transferred to the CoFeB strip and rotates magnetization due to magnetostriction effect. The magnetization rotation is electrically detected by measuring the anisotropic magnetoresistance (AMR) of the CoFeB strip. We decoupled the magnetostriction effect from the piezoresistive contributions, showcasing them as two distinct effects.

MAGNETOELECTRIC TRANSDUCER DESIGN

Figure 1 presents the 3D view of the magnetoelectric MEMS transducer for voltage control of magnetic anisotropy. The device consists of three terminals which are used to bias the cantilever and measure the AMR of ferromagnetic strip. AlN causes the cantilever to bend that generates uniaxial strain on the CoFeB strip. The strain shifts the magnetic anisotropy due to magnetostriction which is measured as a change in the AMR response. AMR is a property of ferromagnetic materials where the resistance of a ferromagnetic strip depends on the angle between direction of electrical current and magnetic field. The resistance of the ferromagnetic strip is expressed as: $R_{FM} = R_{\perp} + (R_{\parallel} - R_{\perp})cos^2\theta$ where θ is the angle between electrical current and magnetic field and $R_{\parallel,\perp}$ are the resistances for $\theta = 0° \; and \; 90°$. The AMR ratio of the ferromagnetic strip is calculated by: $(R_{\parallel} - R_{\perp})/R_{\perp}$.

Thin-film ferromagnet is patterned as a strip and placed along the cantilever length along the x direction (FM easy axis is along x). In the presence of an external field (H_{ext}) in y and cantilever bending in z directions (cantilever bending in z direction generates uniaxial strain along the x axis), effective magnetic field on the ferromagnetic strip can be defined as: $\overrightarrow{H_{eff}} = \overrightarrow{H_{ext}}\hat{y} + (\overrightarrow{H_{an}} + \overrightarrow{H_{mech}})\hat{x}$ where H_{an} is magnetic anisotropy and H_{mech} is the generated field due to magnetostriction effect. The H_{mech} is calculated as [11]: $H_{mech} = 3\beta_{eff}\varepsilon_x/M_s$ where β_{eff} and M_s are magnetostriction coefficient and saturation magnetization for CoFeB and ε_x is strain generated by cantilever bending. Therefore, the resistance of the CoFeB strip can be modulated by preferential bending of cantilever.

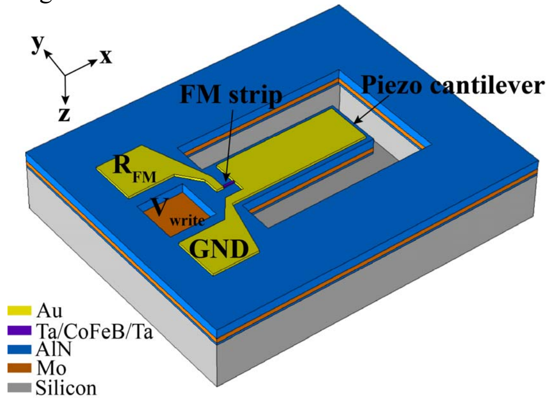

Figure 1: 3D view of magnetoelectric MEMS transducer for voltage control of magnetic anisotropy. The maximum strain is generated at the base by bending the AlN cantilever and the magnetization change is detected by measuring AMR of the FM strip.

FABRICATION

Unpatterned CoFeB thin-films are first characterized by measuring their MH loop in vibrating scanning magnetometer (VSM). Before the film deposition, AlN surface roughness is measured as 4 nm with an atomic force microscopy (AFM). Then, 3 nm Ta/ 20 nm CoFeB / 3 nm Ta film stack is sputtered on 1 µm-AlN coated silicon chips. This chip is diced into 5x5 mm^2 pieces for testing in the VSM where an external magnetic field is applied to the parallel to the CoFeB film surface (easy axis) and the magnetic moment is measured. The magnetization is then calculated by *M=m/V* where *m* is the magnetic moment and *V* is the volume of CoFeB film. Figure 2 presents MH loop of Ta/CoFeB/Ta film stack on AlN film measured by VSM. The 20 nm thick CoFeB film has an in-plane magnetic anisotropy with a saturation magnetization (M_s) of 1057 emu/cm^3 that is very close to previously reported M_s of CoFeB films (1100 emu/ cm^3).

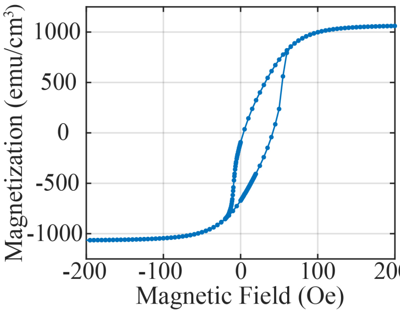

Figure 2: M-H loop of Ta/CoFeB/Ta film stack on AlN measured by VSM. The 20 nm thick CoFeB film has an in-plane magnetic anisotropy with a saturation magnetization (M_s) of 1057 emu/cm^3.

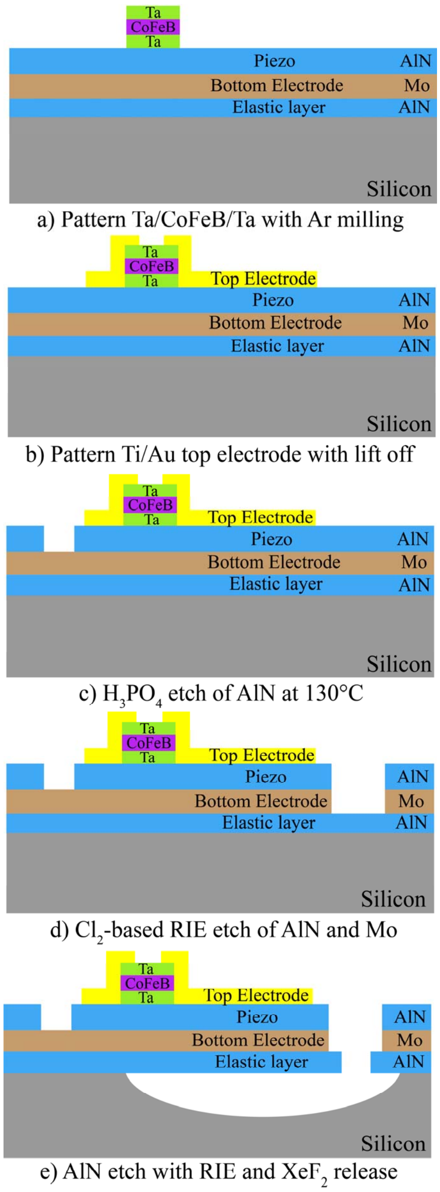

Figure 3: Major fabrication steps of magnetoelectric MEMS transducers.

Once the quality and orientation of the films are verified, same film stack (3 nm Ta/20 nm CoFeB/3 nm Ta) is sputtered on 100 nm AlN/200 nm Mo/1000 nm AlN films on a (100) p-type high-resistive silicon wafer. The top and bottom Ta serve as capping and adhesion layers for the CoFeB film, respectively. The 100 nm thin AlN film is not only used to break the symmetry of the piezoelectric stack for cantilever bending but also to protect the Mo layer during the XeF_2 release step. The Ta/CoFeB/Ta films are patterned as 15:7 µm^2 strips by Ar milling (Figure 3-a). 20 nm Ti/ 100 nm Au thick electrodes are deposited and patterned with e-beam evaporation and lift-off, respectively (Figure 3-b). Next, 1 µm thick AlN layer is wet etched with hot phosphoric acid at 130°C to access bottom electrode where Mo layer serves as an etch stop (Figure 3-c). The cantilever structure is formed by etching 1 µm AlN/ 200 nm Mo with RIE using Cl_2/$BlCl_3$/Ar and Cl_2/O_2 plasma, respectively (Figure 3-d). Finally, 100 nm thick AlN layer is etched with RIE and devices are released in XeF_2 (Figure 4-e). Figure 4 presents the SEM pictures of the fabricated prototypes. The closer view of an AlN cantilever clearly shows that CoFeB strip is located at the anchor of the cantilever. The cantilever has an initial curl-up due to internal material stress of the stack.

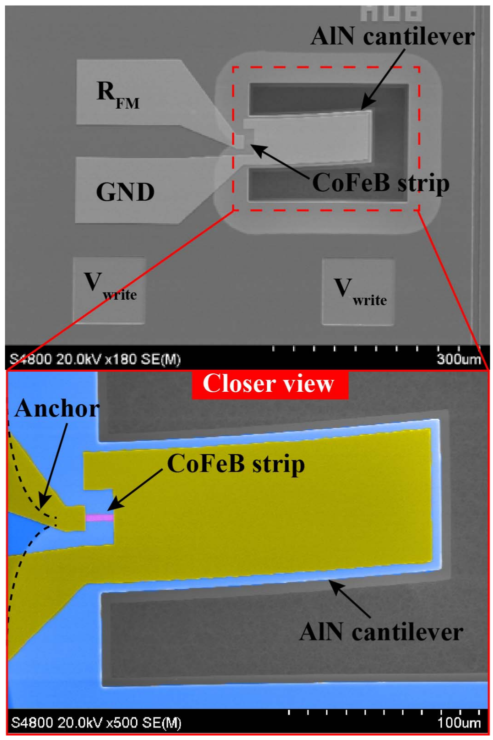

Figure 4: SEM pictures of the fabricated prototypes. Closer view shows the details of a CoFeB strip on AlN cantilever.

MEASUREMENT RESULTS

Laser Doppler Vibrometer (LDV) is an accurate way of measuring tip displacement of cantilevers without any need for a sense electrode. Therefore, AlN cantilevers are characterized using LDV under atmosphere. In this test, cantilevers are excited by applying a positive voltage the bottom electrode while top electrode is grounded. When cantilever is driven using a triangle wave at off-resonance, the DC velocity at the cantilever tip can be optically measured in time domain. The velocity is then integrated to get the maximum displacement. Figure 5 presents measured and simulated DC displacement at the tip of AlN cantilever. Slight difference in the COMSOL and displacement measurements are due to the initial curl-up preventing exact focusing at the cantilever tip. The maximum displacement is used to calculate the maximum in-plane stress at the cantilever base using the expression $\sigma_x = 3E_c t_c X_z / 2L_c^2$ where E_c, t_c and L_c are Young's modulus, thickness, and length of the cantilever and X_z is the maximum deflection of cantilever tip at the z-direction. Assuming cantilever in the linear region at 45V (LDV maximum voltage is 9V), the in-plane strain is calculated to be 270 ppm using $\varepsilon_x = \sigma_x / E_{FM}$ (E_{FM} is the Young's modulus of CoFeB).

Figure 6 presents magneto-transport test setup used to characterize AMR of CoFeB strips. The setup consists of a GMW 3-axis projected magnet capable of generating 3-axis $\pm$ 0.3 Tesla magnetic field with 360° rotation. For the measurement accuracy, magnetic field is calibrated using a 3-axis hall sensor before testing. The resistances of CoFeB strips are measured using Zurich HF2LI lock-in amplifier either by sweeping the in-plane magnetic field along hard axis (θ = 90°) of the CoFeB strip or magnetic fields at different angles.

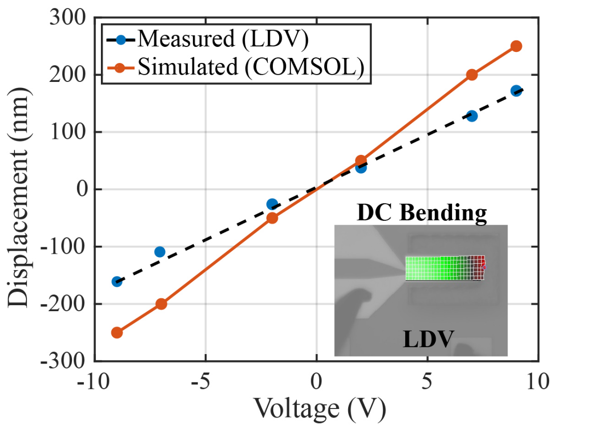

Figure 5: Measured and simulated maximum DC displacement at the tip of AlN cantilever. The maximum tip displacement is used to calculate the in-plane stress at the cantilever base.

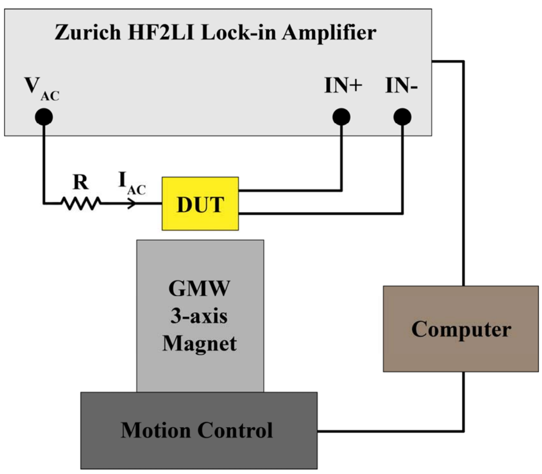

Figure 6: Magneto-transport test setup.

Figure 7 shows the AMR measurements of reference CoFeB strips on the chip. First, magnetic field is swept from negative to positive 1500 Oe and vice versa along hard axis (θ = 90°) of the CoFeB strip and magnetoresistance is measured. The coercivity (H_c) is the half of the distance between two peaks and calculated as 40 Oe. Then magnetic field angle is swept at 1500 Oe from -180 to 180 degrees and the AMR ratio is measured as 0.06%. The measurement results are perfectly fitted to the AMR equation. Figure 8 presents the AMR measurements of CoFeB strips on an AlN cantilever with and without cantilever bending. In this test, first magnetic field is swept from negative to positive 400 Oe along hard axis of the CoFeB strip and magnetoresistance is measured. Then, 45 V is applied to the AlN cantilever and magnetoresistance of the CoFeB is again measured. Biasing the cantilever at 45 V causes an in-plane strain of 270 ppm on CoFeB strip, exhibiting a 22% change in the AMR ratio. This change in the AMR ratio implies a rotation in the magnetic anisotropy by 20°.

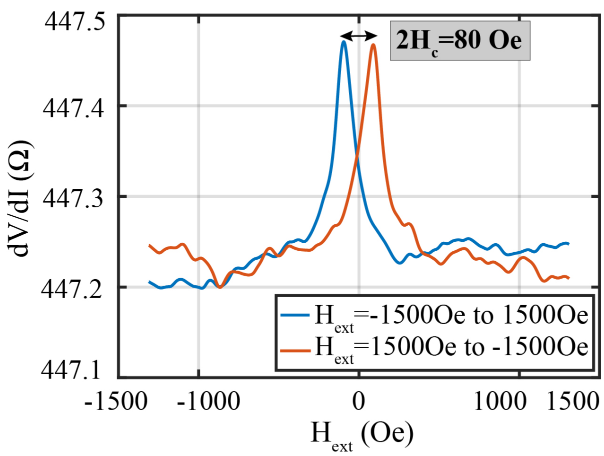

a)

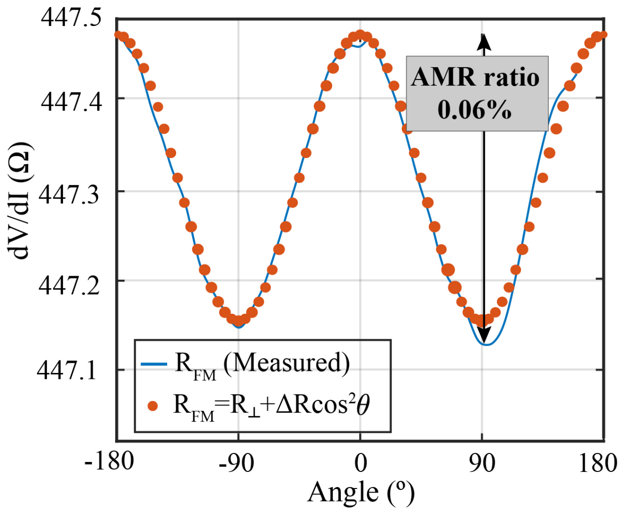

b)

Figure 7: AMR measurements of reference CoFeB strips on the chip: (a) Magnetic field is swept along hard axis (θ = 90°) of the CoFeB strip and magnetoresistance is measured. The AMR ratio is 0.06% and the coercivity is around 40Oe. (b) AMR measurements when magnetic field angle is swept (H_{ext}=1500Oe) and fit to AMR equation.

The magnetostriction coefficient (β_{eff}) is extracted by using: $H_{mech} = 3\beta_{eff}\varepsilon_x/M_s$ where H_{mech} is the field generated due to magnetostriction effect [11]. H_{mech} of 9 Oe causes a rotation of 20° and corresponding β_{eff} is extracted as 1.75 ergs/cm^3, very close to β_{eff} recently reported (4 ergs/cm^3) in [12] for as deposited CoFeB thin-films. There is also a change due to piezoresistance (PZR) effect where the whole AMR curve shifts up/down depending voltage polarity. The gauge factor (*GF*) is calculated as 2.1 by $GF = \Delta R/\varepsilon_x$.

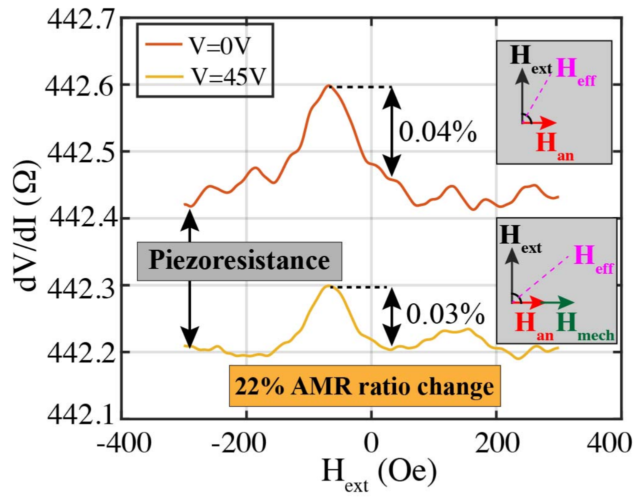

Figure 8: Bending the cantilever at 45V causes an in-plane strain of 270ppm on CoFeB strip and therefore shows a distortion in the AMR peak, exhibiting a 22% change in the AMR ratio and rotates the magnetic anisotropy by 20°.

CONCLUSIONS

This paper presents the first implementation of strain-mediated magnetization using MEMS actuators. Our results demonstrate that magnetic anisotropy of a CoFeB thin-film ferromagnet can be controlled with an AlN cantilever. We decoupled the magnetostriction effect from the piezoresistive contributions, showcasing them as two distinct effects. Overall, these results are the starting point of new class of hybrid devices where low power MEMS actuators can be used to manipulate spintronic systems.

ACKNOWLEDGEMENTS

Authors would like to thank Prof. John Heron, Dr. Kerem Yunus Camsari, Dr. Tanay Arun Gosavi, and Peter Meisenheimer for valuable discussions on the theory, design and fabrication of magnetoelectric MEMS transducers. Authors also would like to thank Semiconductor Research Corporation (SRC) for supporting this research.

REFERENCES

[1] S. Manipatruni, D. E. Nikonov, C. Lin, T. A. Gosavi, H. Liu, B. Prasad, Y. Huang, E. Bonturim, R. Ramesh, I. A. Young, "Scalable energy-efficient magnetoelectric spin-orbit logic," Nature, 565. pp.35-42, 2019.

[2] J. T. Heron, J. L. Bosse, Q. He, M. Trassin, L. Ye, J. D. Clarkson, C. Wang, J. Liu, S. Salahuddin, D. C. Ralph, D. G. Sclom, J. Iniguez, B. D. Huey, and R. Ramesh, "Deterministic switching of ferromagnetism at room temperature using an electric field," Nature 516, pp. 370-373, 2014.

[3] P. B. Meisenheimer, S. Novakov, N. M. Vu, and J. T. Heron, "Perspective: Magnetoelectric switching in thin film multiferroic heterostructures," Journal of Applied Physics, 123, 240901, 2018.

[4] Y. Yang, H. Huang, Z. Luo, C. Gao, X. Li, and C. F. Tao, "Electric-field control of magnetic anisotropy rotation in multiferroic Ni/(011)-$Pb(Mg_{2/3}Nb_{1/3})_{0.7}Ti_{0.3}O_3$ heterostructures," Journal of Applied Physics, 122, 134105, 2017.

[5] W. Zhou, C. Ma, Z. Gan, Z. Zhang, X. Wang, W. Tan, and D. Wang, "Manipulation of anisotropic magnetoresistance and domain configuration in Co/PMN-PT (011) multiferroic heterostructures by electric field," Applied Physics Letters 111, 052401, 2017.

[6] K. Cai, M. Yang, H. Ju, S. Wang, Y. Ji, B. Li, K. W. Edmonds, Y. Sheng, B. Zhang, N. Zhang, S. Liu, H. Zheng, and K. Wang, "Electric field control of deterministic current-induced magnetization," Nature Materials, Vol.16, pp.712-717, 2017.

[7] A. Chen, Y. Wen, B. Fang, Y. Zhao, Q. Zhang, Y. Chang, P. Li, H. Wu, H. Huang, Y. Lu, Z. Zeng, J. Cai, X. Han, T. Wu, X. Zhang, and Y. Zhao, "Giant nonvolatile manipulation of magnetoresistance in magnetic tunnel junctions by electric fields via magnetoelectric coupling," Nature communications, 10 (1), 243, 2019.

[8] A. K. Biswas, H. Ahmad, J. Atulasimha, and S. Bandyopadhyay, "Experimental demonstration of complete 180 reversal of magnetization in isolated Co nanomagnets on a PMN-PT substrate with voltage generated strain," Nanoletters 17 (6), pp. 3487-3484, 2017.

[9] J. Irwin, S. Lindemann, W. Maeng, J. J. Wang, V. Vaithyanathen, J. M. Hu, L. Q. Chen, D. G. Schlom, C. B. Eom, and M. S. Rzchowski, "Magnetoelectric coupling by giant piezoelectric tensor design," arxiv:1901.02456, 2019.

[10] B. Jiang, N. Opondo, G. Wolfowicz, D. D. Awschalom, and S. A. Bhave, "SiC cantilevers for generating uniaxial stress," Solid State Sensors, Actuatros and Microsystems (Transducers'19), pp. 1655-1658, 2019.

[11] M. M. Torunbalci, T. A. Gosavi, K. Y. Camsari and S. A. Bhave, "Magneto acoustic spin hall oscillators," Scientific Reports 8, no.1, pp.1119, 2018.

[12] P. G. Gowtham, G. M. Stiehl, D. C. Ralph, and R. A. Buhrman, "Thickness-dependent magnetoelasticity and its effects on perpendicular magnetic anisotropy in Ta/CoFeB/MgO thin films," Physical Review B, 93, 024404, 2016.

CONTACT

*M. M. Torunbalci, tel: +1-765-418-8559; mtorunba@purdue.edu